Article

Understanding the Barriers to Crystal Growth: Dynamical Simulation of the Dissolution and Growth of Urea from Aqueous Solution

Stefano Piana, and Julian D. Gale

J. Am. Chem. Soc., **2005**, 127 (6), 1975-1982• DOI: 10.1021/ja043395l • Publication Date (Web): 20 January 2005

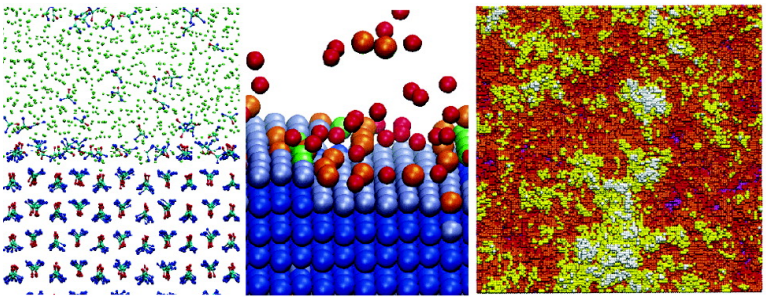

J|A|C|S
ARTICLES
Published on Web 01/20/2005

Understanding the Barriers to Crystal Growth: Dynamical Simulation of the Dissolution and Growth of Urea from Aqueous Solution

Stefano Piana and Julian D. Gale*

Contribution from the Nanochemistry Research Institute, Department of Applied Chemistry, Curtin University of Technology, P.O. Box U1987, Perth 6845, Western Australia

Received November 2, 2004; E-mail: julian@power.curtin.edu.au

Abstract: Both the dissolution and growth of a molecular crystalline material, urea, has been studied using dynamical atomistic simulation. The kinetic steps of dissolution and growth are clearly identified, and the activation energies for each possible step are calculated. Our molecular dynamics simulations indicate that crystal growth on the [001] face is characterized by a nucleation and growth mechanism. Nucleation on the [001] urea crystal face is predicted to occur at a very high rate, followed by rapid propagation of the steps. The rate-limiting step for crystallization is actually found to be the removal of surface defects, rather than the initial formation of the next surface layer. Through kinetic Monte Carlo modeling of the surface growth, it is found that this crystal face evolves via a rough surface topography, rather than a clean layer-by-layer mechanism.

Introduction

The dissolution and growth of crystals from solution are very important fundamental processes in chemistry. In the pharmaceutical industry, for instance, crystal growth and polymorphism are key properties that must be controlled during preparation. Despite this, our understanding of exactly how crystals grow at an atomistic level is still far from complete. The aim of the present work is to address this deficiency, at least for the case of a fast-growing molecular crystalline system.

A large number of studies have been devoted to determining the factors that control the morphology and purity of crystals grown from liquid solutions. From these studies, several models have been developed to relate crystal lattices to crystal morphologies. The simplest models relate the degree of representation of a particular cleavage surface to the density of the planes perpendicular to the face.[1−3] More sophisticated models take into account the explicit atomic structure and relaxation of the surface structure. Here two general approaches exist. In the first, the surface energy (i.e., the thermodynamic cost of creating the surface) is used to determine the crystal morphology via a Wulff construction.[4] The second method is to determine the attachment energies of surface layers to the crystal faces.[5,6] Although both methods are strictly thermodynamic assessments of the tendency to form particular surfaces, the latter approach is often viewed as being representative of the crystal morphology when grown under kinetic control, since faces where the energy of addition of a further layer is more exothermic should grow faster. However, this hypothesis neglects to take into account the fact that the rate of desolvation may be the determining factor, rather than incorporation into the surface. The effect of solvent and impurities on the relative stability of the faces can be included in these calculations, either explicitly or implicitly, and has been shown to improve the accuracy of these models.[7] However, none of these approaches explains the detailed mechanism by which the crystal grows.

As crystallization is intrinsically a nonequilibrium process, the crystal morphology can be dominated by the kinetics of crystal growth. The largest faces are the slowest to grow, while the smallest faces are the fastest. Models based on thermodynamic considerations are only successful in predicting crystal morphologies since it is often the case that the slowest growing faces are also the most stable. However, there are exceptions to this and thus the great diversity of morphologies that can be observed for many materials. Unfortunately, the characterization of the individual steps of crystal growth and dissolution at the atomic level of resolution are not easy tasks. Sometimes the kinetics of crystal growth can be inferred by inspection of a growing face with electron or atomic force microscopy. These studies have shown that, in most cases, crystal faces grow by propagation of steps originating from a growth nucleus. Where nucleation is kinetically very slow, growth may occur from screw dislocations, giving rise to characteristic spiral patterns that can be observed with microscopy.

The growth of urea crystals has attracted considerable attention in recent years because of the importance of obtaining pure urea crystals for exploiting the nonlinear optic properties of this material. In addition, it is relatively easy to grow urea

(1) Bravais, A. *Etudes Cristallographiques*; Gauthiers-Villars: Paris, 1886.
(2) Friedel, M. G. *Bull. Soc. Fr. Mineral.* **1907**, *30*, 326−455.
(3) Donnay, J. D. H.; Harker, D. *Am. Mineral.* **1937**, *22*, 446−467.
(4) Kern, R. The Equilibrium Form of a Crystal. In *Morphology of Crystals*; Sunagawa, I., Ed.; Terra Scientific Publishing (TERRAPUB): Tokyo, 1987; pp 77−206.
(5) Hartman, P.; Bennema, P. *J. Cryst. Growth* **1980**, *49*, 145−156.
(6) Hartman, P.; Perdok, W. G. *Acta Crystallogr.* **1954**, *8*, 49−52.
(7) Winn, D.; Doherty, M. *AIChE J.* **2000**, *46*, 1348−1367.

10.1021/ja043395l CCC: $30.25

crystals of several centimeters in size from a supersaturated solution within a few hours. Therefore, the process is very well-suited to being studied with experimental techniques because of its rapidity. Urea grows from supersaturated aqueous, or methanol, solutions as needlelike crystals with dominant [110] faces. The fastest growing faces are the [001] and, to a lesser extent, the [111]. The morphology of vapor-grown urea crystals can be satisfactorily predicted from the aforementioned attachment energies.[8,9] However, these methods severely underestimate the [001] to [110] ratio (about 20 to 50) observed when crystals are grown from solution.[8]

In principle, molecular dynamics (MD) simulations are an ideal tool to characterize the energetics and structural features of the individual steps of crystal growth from a solution at the atomic level of resolution. However, for most materials the physical time scale required to observe significant growth of a crystal surface is too long to be accessible to direct simulation. Consequently, the majority of studies of crystal growth performed to date have been performed with kinetic Monte Carlo methods.[10] Here the rate constants for processes are typically determined statically, through transition-state theory, and then the system is propagated on the basis of an event table that is often precomputed, though it can also be determined on the fly.[11] This approach is appropriate when the activation energies are high and most readily performed for the situations such as modeling of molecular beam expitaxy where there is no solvent to complicate the identification of possible pathways. It also is rendered approximate by virtue of the fact that activation energies are computed and then prefactors have to be estimated to predict the rate of processes.

Molecular dynamics simulation has been applied to alloys and metals, as well as model systems with simple interaction parameters, such as Lennard-Jones fluids[12,13] Recently, it has even been applied to the formation of small NaCl[14,15] and AgBr[16] crystal nuclei from aqueous solution. However, to the best of our knowledge, no MD simulation of the dissolution or growth of a molecular crystal has been reported in the literature so far, probably because the larger number of degrees of freedom for organic molecules that must be sampled makes the calculation computationally challenging.

In the present work, the aim is to examine both the dissolution and growth of a molecular crystalline material for the first time. For this purpose, we have chosen to study urea as an example for two reasons: (i) the urea molecule has no facile torsional degrees of freedom, and therefore sampling of the conformation space is simplified and (ii) urea is known to grow very rapidly from an experimental point of view, which maximizes the probability of observing significant events on a time scale that is accessible to current dynamical simulations.

MD simulations have already been used to study the orientation and diffusion of urea molecules on the urea crystal faces in contact with solution.[17] From this study, the rate of reorientation of urea molecules on the crystal surface has been calculated and used to estimate the relative rate of kink incorporation for different faces of the urea crystal.[18] This was performed on the basis of the assumption that growth originated from a screw dislocation and that incorporation of growth units in the step is rate-limiting. Here we go further and report the molecular dynamics simulation of the actual dissolution and growth of the [001] urea crystal face from aqueous solution, this surface being chosen as the fastest growing one of morphological importance. The kinetic processes leading to dissolution and growth were identified, without prior assumptions, and the rates for each possible step were determined. These values were then used as the basis of a kinetic Monte Carlo calculation of the growth of the urea [001] surface to extend the simulations to much greater time and length scales.

Methods

In the present work, we performed molecular dynamics simulations using an atomistic approach, with a force field description of the interactions between atoms. Parameters for urea were taken from previous work by Duffy et al.[19,20] These parameters have recently been carefully evaluated and are found to provide an accurate description of the energy of dissolution of urea from the gas phase into an SPC model for water.[20] Furthermore, the urea sublimation enthalpy calculated with these parameters (92.4 kJ mol^{-1}) is very close to the experimental sublimation enthalpy (93.5 kJ mol^{-1}).[21] Because this combined force field has been found to yield such good results, we have employed the same parameters for urea, the urea−water interaction, and the SPC model to represent water. The initial starting coordinates for the [001] surface were generated from the unit cell of urea as determined by X-ray diffraction.[22] The program GDIS[23] was used to construct 2-D periodic surfaces of urea. Two distinct systems with different surface areas were built: surface 1, which consisted of an 8×8 supercell, and surface 2, comprising a 5×5 supercell. The depths of the urea slabs were 6 and 10 unit cells, respectively. These 2-D cells were then converted into 3-D cells, with the *c*-axis perpendicular to the *a* and *b* surface vectors with a magnitude 25 Å larger than the thickness of the surface slab. In this way, two [001] surfaces were present in the 3-D cell. The 25 Å gap between the two surfaces was filled with water molecules using the genbox package within GROMACS.[24] The final systems consisted of 768 urea molecules and 1295 water molecules for surface 1 and 500 urea molecules and 761 water molecules for surface 2.

Molecular dynamics simulations were performed on the two systems in the isothermal, isobaric (NPT) ensemble using the program GROMACS.[24] The systems were coupled to a Berendsen thermostat with a relaxation time of 4.0 ps and a Berendsen barostat[25] with a relaxation time of 5.0 ps. The time step for the simulations was 2.0 fs. Nonbonded interactions were calculated with a cutoff of 9.0 Å. The particle mesh Ewald (PME) method[26,27] was used for treating the long-range electrostatic interactions. All simulations were equilibrated for 200 ps

(8) Brunsteiner, M.; Price, S. L. *Cryst. Growth Des.* **2001**, *1*, 447−453.
(9) Engkvist, O.; Price, S. L.; Stone, A. J. *Phys. Chem. Chem. Phys.* **2000**, *2*, 3017−3027.
(10) Jónsson, H. *Annu. Rev. Phys. Chem.* **2000**, *51*, 623−653.
(11) Henkelman, G.; Jónsson, H. *J. Chem. Phys.* **2001**, *115*, 9657−9666.
(12) Paik, S. M.; Das Sarma, S. *Phys. Rev. B* **1989**, *39*, 1224−1228.
(13) Anwar, J.; Boateng, P. K. *J. Am. Chem. Soc.* **1998**, *120*, 9600−9604.
(14) Zahn, D. *Phys. Rev. Lett.* **2004**, *92*, 040801.
(15) Mucha, M.; Jungwirth, P. *J. Phys. Chem. B* **2003**, *107*, 8271−8274.
(16) Shore, J. D.; Perchak, D. *J. Chem. Phys.* **2000**, *113*, 6276−6284.
(17) Boek, E. S.; Briels, W. J.; Feil, D. *J. Phys. Chem.* **1994**, *98*, 1674−1681.
(18) Liu, X. Y.; Boek, E. S.; Briels, W. J.; Bennema, P. *Nature* **1995**, *374*, 342−345.
(19) Duffy, E. M.; Severance, D. L.; Jorgensen, W. L. *Isr. J. Chem.* **1993**, *33*, 323−330.
(20) Smith, L. J.; Berendsen, H. J. C.; Van Gusteren, W. F. *J. Phys. Chem. B* **2004**, 1065−1071.
(21) Ferro, D.; Barone, G.; Della Gatta, G.; Piacente, V. *J. Chem. Thermodyn.* **1987**, *19*, 915−923.
(22) Swaminathan, S.; Craven, B. M.; Spackman, M. A.; Stewart, R. F. *Acta Crystallogr.* **1984**, *B40*, 398−404.
(23) Fleming, S. D.; Rohl, A. L. GDIS. *Z Kristallogr.*, in press.
(24) Lindhal, E.; Hess, B.; van der Spoel, D. *J. Mol. Model.* **2001**, *7*, 306−317.
(25) Berendsen, H. J. C.; Postma, J. P. M.; Van Gusteren, W. F.; DiNola, A.; Haak, J. R. *J. Chem. Phys.* **1984**, *81*, 3684−3690.
(26) Darden, T. A.; York, D. *J. Chem. Phys.* **1993**, *98*, 10089−10094.
(27) Essman, U.; Perera, L.; Berkowitz, M. L.; Darden, T. A.; Lee, H.; Pedersen, L. G. *J. Chem. Phys.* **1995**, *103*, 8577−8593.

prior to data acquisition, during which energies, cell parameters, and coordinates were sampled after every 1 ps. An anisotropic pressure coupling was used in the present work. This pressure coupling is more appropriate for the study of a system with both a crystal and a liquid phase. In these simulations, the *x* and *y* cell directions are determined by the crystal lattice and are not expected to change much after equilibration, while the *z* direction should adjust to changes in the liquid-phase composition as the dissolution and crystallization reactions proceed. In preliminary MD simulations of bulk urea, with the model adopted in the present work, a distortion of the lattice vectors (a +15%, b −13%) is observed after a few hundred picoseconds. This distortion is not observed if an isotropic pressure coupling is used. For this reason, a control simulation of dissolution and growth has also been performed with an isotropic pressure scaling. This simulation gave essentially the same results in term of reaction rates and activation energies, as in the anisotropic case. Hence, while the distortion of the urea structure under ambient conditions is a deficiency of the potential model for urea, it has negligible influence on the aqueous interface and crystal dissolution process.

Several MD simulations at 298 and 260 K were carried out to assess the reproducibility of the results with respect to the size of the simulation cell and conditions. All the simulations under the same conditions of temperature and pressure gave very similar results. For this reason, only one simulation at 298 K and one simulation at 260 K are discussed in detail, as they are representative of the observations in all cases. However, the quantitative values for the crystal growth and dissolution kinetic steps have been calculated as averages over all of the simulations carried out to ensure the best possible statistics, and standard deviations are indicated where relevant. Full details regarding all the MD simulations are given below.

Two MD simulations were performed at 298 K starting from the same initial coordinates of surface 1. Simulations 1a and 1b were carried out for 12 ns with the same parameters, but with different random starting velocities. A single 70-ns MD simulation at 298 K was performed for surface 2; this simulation was divided in two parts (simulation 2a and simulation 2b) during data analysis. Two MD simulations were carried out starting from the final structure obtained from simulations 2a and 2b. In this second set of simulations, the temperature was lowered from 298 to 260 K during 2 ns of simulated annealing, and then a further 38 ns of molecular dynamics at 260 K was performed.

In all of the above simulations, crystal dissolution and growth are free to occur as the conditions dictate. However, an alternative strategy for the study of crystal dissolution would be to examine the activation free energy based on a constrained simulation in which a single molecule of urea is forced from the nondefective surface into solution. Three constrained MD simulations at 298 K were performed to compare this approach with the results of the unbiased dynamics. Here a single urea molecule from a perfect [001] crystal surface was extracted using surface model 1. The distance between the center of mass of the molecule and the surface was constrained, and the constraint distance was smoothly increased from 0 to 2 Å. The relative free energy was calculated as the integral of the constraint force. Three different rates of constraint distance increase were used: 5, 2, and 1 Å ns^{-1}.

To characterize the crystal dissolution and growth process, it is convenient to divide the urea molecules into "crystal-like" and "non crystal-like" molecules, as well as further subdivisions that describe more specifically the local environment of a given molecule. This is illustrated schematically in Figure 1. This kind of subdivision is somewhat arbitrary, and care should be taken to evaluate the dependence of the results on the method used to define which molecules are considered part of the crystal and which are not. In this work, crystalline urea molecules were defined as those having the C−O axis within 25° of the *z*-axis, which represents the direction of the surface normal as well as the bulk orientation, and a C−O axis diffusion cone <25°. The orientation of the C−O axis and the diffusion cone were calculated

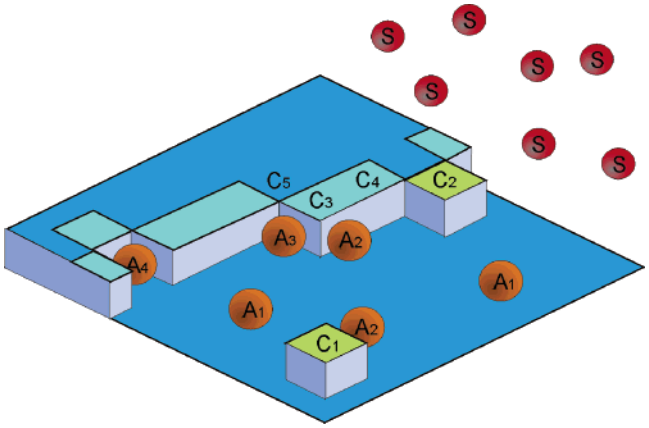

Figure 1. Schematic illustration of the Kossel model in which the growth of a crystal layer proceeds stepwise. Molecules are transported from the solution to the crystal surface, where they diffuse and are eventually integrated into the growing step at the kink sites. Within this model, molecules can be divided into solution molecules (S), molecules adsorbed on the crystal surface (A), and crystal-like molecules (C). Adsorbed and crystalline molecules can be further classified according to the number of contacts they have with the crystal surface. Within this scheme, a C_6 molecule is a crystalline molecule with six contacts, corresponding to a bulk molecule, while a C_4 molecule is one situated at a step. In the same way, an A_1 molecule is one adsorbed on the planar crystal surface, while an A_3 molecule is one adsorbed at a kink site.

at 50-ps intervals. If the same analysis is performed using either 100-ps intervals or a tolerance of 20° for the cone angle, essentially the same results are obtained. It should be pointed out that rotation freedom is not the only possible way to discriminate between crystal-like and non-crystal molecules. Translation freedom is another obvious choice, as crystal molecule are expected to show negligible diffusion. This would lead to a slightly different, but equally valid, categorization. The crystal-like molecules were further subdivided in C_1, C_2, C_3, C_4, C_5, C_6 according to the number of neighboring crystal molecules, to characterize the local environment. The cutoff for the neighbor search was 4.2 Å within the *x*-*y* plane and 5.0 Å along the *z*-axis. For urea, within this definition, C_6 corresponds to a molecule in the bulk crystal, C_5 is a molecule situated within a planar surface, C_4 is a molecule within a step, and C_3 is a molecule at a kink.

The noncrystalline molecules were further divided into solution and adsorbed molecules. Adsorbed molecules were defined as noncrystalline molecules with at least one contact with a $C_{(2-6)}$ molecule and also subdivided into A_{1-5} according to the number of crystal-like neighbors. Within this definition, an A_1 molecule is a molecule adsorbed on a nondefective surface, while an A_2 molecule is one that is adsorbed at a step, and an A_3 molecule is one that is adsorbed at a kink.

Finally, empty sites on the crystal surface were defined as sites 4.7 Å above a $C_{(2-5)}$ surface molecule. Empty sites were also subdivided in S_{1-5} according to the number of crystal neighbors, as per the adsorbed molecules. Within this definition, an S_1 position is a vacant site on a planar nondefective face of the crystal, while an S_4 site is a vacancy in a step, and an S_5 site is a vacancy in a face.

Transition rates k^{50}_{a-b} (Table 1) were calculated from the average number of events n^{50}_{a-b} in a 50-ps time frame according to one of two expressions:

$$k^{50}_{a-b} = \frac{1}{50 \times 10^{-12}} \frac{\langle n^{50}_{a-b} \rangle}{\langle a \rangle}$$

where $\langle a \rangle$ is the MD average number of molecules of type *a*, and it applies except in the case of the reaction with an empty surface site, in which case the equation becomes:

Table 1. Rate Constants (M^{-1} s^{-1}) Calculated from the MD Simulations[a]

	S	A_1	A_2	A_3	A_4	A_5	C_1	C_2	C_3	C_4	C_5	C_6
S	−	5.9e+09	8.0e+09	2.6e+09	7.0e+08	2.3e+08	1.2e+09	3.3e+09	1.5e+09	6.1e+08	1.1e+08	−
A_1	1.0e+10	3.2e+09	7.7e+09	4.5e+09	1.6e+09	7.2e+08	6.0e+08	−	−	−	−	−
A_2	3.6e+09	1.4e+09	8.4e+09	6.5e+09	2.5e+09	2.3e+09	−	1.6e+09	-	−	−	−
A_3	8.2e+08	6.7e+08	4.2e+09	3.6e+09	2.5e+09	4.5e+09	−	−	4.2e+09	−	−	−
A_4	1.3e+08	2.2e+08	2.8e+09	1.8e+09	4.0e+09	7.7e+09	−	−	−	6.2e+09	−	−
A_5	8.6e+06	3.0e+07	6.0e+08	1.4e+09	2.4e+09	2.6e+09	−	−	−	−	8.2e+09	−
C_1	5.1e+09	1.7e+09	−	−	−	−	−	−	−	−	−	−
C_2	8.0e+08	−	1.2e+09	−	−	−	−	−	−	−	−	−
C_3	1.6e+08	−	−	1.1e+09	−	−	−	−	−	−	−	−
C_4	7.5e+06	−	−	−	7.4e+08	−	−	−	−	−	−	−
C_5	1.0e+06	−	−	−	−	5.6e+08	−	−	−	−	−	−
C_6	−	−	−	−	−	−	−	−	−	−	−	−

[a] S represents solute urea molecules; A_{1-5} are urea molecules adsorbed on the surface, and C_{1-6} are crystal-like molecules (see full discussion in the Methods section).

$$k_{a-b}^{50} = \frac{1}{50 \times 10^{-12}} \frac{\langle n_{a-b}^{50} \rangle}{\langle a \rangle \langle [b] \rangle}$$

where $[b]$ is the fraction of empty sites of type b on the crystal surface. Events $a-b$ are identified as specific events where one molecule classified as type a changes to type b in the subsequent time frame.

For molecules in solution, the mean number of molecules was calculated as the average number of dissolved molecules within 5 Å from the adsorbed layer. Activation energies ΔG_{a-b}^{*} (Table 2) were calculated from the expression:

$$\Delta G_{ab}^{*} = k_B T \ln \frac{k_{a-b}^{50}}{\nu^{50}}$$

where ν^{50} is the frequency of diffusion over a barrier of 0 energy. For the steps of incorporation into the crystal lattice and the reverse steps, $\nu^{50} = 50/\tau_3$, where τ_3 is the reorientation correlation time (5 ps).[28] For the other reactive events, it is equal to $\nu^{50} = 50.2D/L^2$, where D is the diffusion coefficient for urea in water, as calculated from the MD simulation, and L is the distance between two adjacent sites. This corresponds to the assumption that the transition state is located midway between the reacting sites.

Relative free energies ΔG_{a-b} (Table 3) were calculated from the direct and inverse rate constants:

$$\Delta G_{ab} = k_B T \ln \frac{k_{a-b}^{50}}{k_{b-a}^{50}}$$

Finally, periodic lattice simulations with a kinetic Monte Carlo algorithm were performed with unit cell sizes ranging from 8 × 8 to 150 × 150. In these simulations, each site and molecule adsorbed on the surface is evolved according to the matrix of transition probabilities calculated from the molecular dynamics simulations. Results for 8 × 8 and 150 × 150 simulations are presented.

Results and Discussion

Urea is highly soluble in water; 1 L of saturated solution at 298 K contains about 570 g of dissolved urea, corresponding to a concentration of approximately 11 M. The concentration of the saturated solution at 298 K, according to our calculations with the present model, ranges between 7 and 11.6 M, in good agreement with this experimental value. Despite this high concentration, the enthalpy of dissolution ΔH_s is positive (13.8 kJ mol^{-1}),[29] indicating that, as in many cases, the dissolution process is driven by the large entropic contribution to the Gibbs free energy ($\Delta S_s = 69.4$ J mol^{-1} K^{-1}).[29] The urea [001] surface is the fastest growing face in solution, producing needlelike crystals with a 20:1 to 50:1 [001]/[110] area ratio. This face is also expected to dissolve readily in aqueous solution at 298 K. To study the dissolution process, NPT molecular dynamics simulations at 1 atm and 298 K were performed on [001] urea crystal surfaces in water. Two different systems were utilized containing 8 × 8 (surface 1) and 5 × 5 (surface 2) unit cells. Two simulations, lasting for 12 ns, were performed for surface 1, while a single 70-ns run was carried out for surface 2 (see Method section). Because the results of all the above simulations are qualitatively very similar, only the results for surface 2 are discussed in detail.

The urea molecules were divided into "crystal-like" and "non crystal-like" molecules, as previously described in the Methods section. This subdivision provides an indicator for the processes that are occurring and makes it possible to define the kinetic steps of the crystal dissolution and growth in term of a Kossel-like scheme (Figure 1). Representative samples of the molecular structure during the dissolution process are shown in Figure 2a−c, while the fractional change in the number of layers of urea molecules as a function of time is reported in Figure 2d. The plot shows that dissolution proceeds in a stepwise fashion until two layers are completely dissolved. At this point, an equilibrium situation is reached and no more dissolution is observed. The final concentration of the solution in the MD simulation of surface 2 is ∼7 M, as compared to the saturated solution experimental value of 11 M at 298 K. While the calculated value is slightly below the experimental one, at this concentration it is possible that dissolution becomes so slow that it is no longer observed within the simulation time. In the MD simulations of surface 1, dissolution is observed until the solution reaches a concentration of 11.6 M.

To understand the individual steps leading to dissolution, each urea molecule has been represented as a ball positioned at the center of mass of the molecule and colored according to the type (see also Figure 1 and caption of Figure 2). Within this representation, it becomes apparent that the dissolution begins with the formation of a few defects on the crystal surface (Figure 2, parts a and a1). As these defects reach a critical size, a fast dissolution of an entire layer is observed (Figure 2, parts b and b1). In the last part of the simulation, the layer is completely dissolved and the solution is now almost saturated with urea molecules. Hence, no further dissolution is observed (Figure 2, parts c and c1). Note that the final number of dissolved layers

(28) Idrissi, A.; Bartolini, P.; Ricci, M.; Righini, R. *Phys. Chem. Chem. Phys.* **2003**, *5*, 4666−4671.
(29) Pickering, M. *J. Chem. Educ.* **1987**, *64*, 723−724.

Table 2. Relative Free Energies (kJ mol^{-1}) Calculated from the Molecular Dynamics Simulations, with Standard Deviations Given in Parenthesis[a]

	S	A_1	A_2	A_3	A_4	A_5	C_1	C_2	C_3	C_4	C_5	C_6
S	–	1.4(0.7)	−1.8(1.7)	−2.5(1.1)	−3.6(1.9)	−6.4(−)	−3.6(1.2)	−2.8(2.1)	−5.4(2.8)	−10.0(3.0)	−10.0(2.7)	–
A_1	−1.4(0.7)	–	−3.8(2.4)	−4.3(1.9)	−4.7(1.9)	−8.0(1.6)	2.3(0.5)	–	–	–	–	–
A_2	1.8(1.7)	3.8(2.4)	–	−1.5(1.5)	0.4(1.5)	−2.5(0.7)	–	−0.8(0.8)	–	–	–	–
A_3	2.5(1.1)	4.3(1.9)	1.5(1.5)	–	−0.5(2.2)	−4.2(1.2)	–	–	−3.1(0.5)	–	–	–
A_4	3.6(1.9)	4.7(1.9)	−0.4(1.5)	0.5(2.2)	–	−2.0(0.9)	–	–	–	−5.5(2.0)	–	–
A_5	6.4(−)	8.0(1.3)	2.5(0.5)	4.2(1.1)	2.0(0.6)	–	–	–	–	–	−6.8(1.5)	–
C_1	−3.6(1.2)	−2.3(0.5)	–	–	–	–	–	–	–	–	–	–
C_2	2.8(2.1)	–	0.8(0.8)	–	–	–	–	–	–	–	–	–
C_3	5.4(2.8)	–	–	3.2(0.5)	–	–	–	–	–	–	–	–
C_4	10.4(3.0)	–	–	–	5.5(2.0)	–	–	–	–	–	–	–
C_5	10.0(2.7)	–	–	–	–	6.8(1.5)	–	–	–	–	–	–
C	–	–	–	–	–	–	–	–	–	–	–	–

[a] S represents solute urea molecules; A_{1-5} are urea molecules adsorbed on the surface, and C_{1-6} are crystal molecules.

Table 3. Activation Energies (kJ mol^{-1}) Calculated from the Molecular Dynamics Simulations, with Standard Deviations Given in Parenthesis[a]

	S	A_1	A_2	A_3	A_4	A_5	C_1	C_2	C_3	C_4	C_5	C_6
S	–	2.7(1.1)	2.2(0.9)	4.8(0.7)	8.2(1.2)	10.6(2.2)	6.7(1.9)	4.6(1.5)	6.2(1.1)	8.3(1.2)	11.6(1.8)	-
A_1	1.3(0.5)	5.7(1.0)	3.9(1.1)	5.2(0.9)	7.5(1.2)	9.5(2.9)	17.7(0.8)	–	–	–	–	–
A_2	3.9(0.9)	7.7(1.5)	3.8(1.2)	4.4(1.1)	6.7(2.0)	6.9(2.4)	–	15.5(0.9)	–	–	–	–
A_3	7.4(0.8)	9.5(1.5)	5.9(2.3)	5.8(1.9)	6.6(2.2)	5.5(2.5)	–	–	13.2(0.7)	–	–	–
A_4	11.8(1.4)	12.2(1.7)	6.1(0.9)	7.1(2.3)	4.8(1.9)	3.9(2.8)	–	–	–	12.3(0.6)	–	–
A_5	18.0(2.5)	17.6(3.7)	9.4(2.0)	8.9(4.0)	6.4(2.0)	1.3(1.4)	–	–	–	–	11.6(0.4)	–
C_1	3.1(1.0)	15.4(0.7)	–	–	–	–	–	–	–	–	–	–
C_2	7.4(0.9)	–	16.3(1.1)	–	–	–	–	–	–	–	–	–
C_3	11.5(1.9)	–	–	16.4(1.1)	–	–	–	–	–	–	–	–
C_4	19.0(2.5)	–	–	–	17.8(2.3)	–	–	–	–	–	–	–
C_5	23.4(2.0)	–	–	–	–	18.4(1.2)	–	–	–	–	–	–
C	–	–	–	–	–	–	–	–	–	–	–	–

[a] S represents solute urea molecules; A_{1-5} are urea molecules adsorbed on the surface, and C_{1-6} are crystal molecules.

is two, which corresponds to one layer per exposed surface. This happens because the system is 3-D periodic, and although we show only one in the pictures for sake of clarity, two [001] surfaces are present in the simulation, one on each side of the slab.

The dissolution enthalpy per molecule can be obtained from the slope of the potential energy versus the number of dissolved urea molecules, as shown in Figure 3. The calculated value of 13.7(0.1) kJ mol^{-1} is in excellent agreement with the experimental value (13.8 kJ mol^{-1}).[29] A more appropriate treatment requires a correction to account for the variation of the concentration of the solution. However, this correction is expected to be ∼1 kJ mol^{-1},[20] and the scatter of the data does not allow it to be estimated with sufficient accuracy.

After 25 ns of MD simulation, the solution concentration remains constant (Figure 2d). However, the formation of metastable crystal nuclei on the surface is observed during the MD simulation. Figure 4 shows the formation of a nucleus of about 12 molecules after 40 ns of MD simulation (Figure 4b). This nucleus is stable for ∼2 ns (Figure 4d) and then dissolves again (Figure 4c). This finding suggests that, in a saturated or supersaturated solution, nucleation on the [001] face should occur at a reasonably high rate. Thus, it should be possible, by simply decreasing the temperature, to simulate the process of nucleation and growth. We performed such a simulation of crystal growth by decreasing the temperature to 260 K during 1 ns of simulated annealing, followed by a further 38 ns of molecular dynamics. After a short induction period (Figure 5d), formation of a nucleus on the crystal face is observed (Figure 5a). During the following 25 ns, the nucleus expands (Figure 5b) until an almost complete new layer is formed on the crystal surface and a new stationary state is reached (Figure 5c). The whole process closely resembles the inverse of the crystal dissolution, although somewhat missing the stepwise character observed previously.

An important observation is that nucleation appears not to be the rate-limiting step for crystal growth on the [001] surface of urea, since, as the above results show, this occurs quite readily even before the temperature is lowered to decrease the supersaturation threshold. It appears that the slowest phase of the crystal growth process is actually the completion of a full layer of urea molecules. The surface layer grows rapidly until a region remains on the surface where water molecules have the appearance of being contained within a surface pit. Removal of such remaining surface defects appears to be rate-limiting. It could be argued that the deceleration of crystal growth observed in the present simulations, as the run progresses, is due to the diminishing degree of supersaturation. However, it is highly likely that this effect would persist even if the supersaturation level were to remain constant. Evidence for this comes from kinetic Monte Carlo simulations that will be presented below, during which the solution concentration of urea can be arbitrarily manipulated.

To fully characterize the kinetic steps of dissolution and growth, the urea molecules were subdivided into crystal-like (C), adsorbed (A), and solution (S). Crystal-like molecules were defined as molecules oriented along the *z*-axis that are not free to rotate and are adjacent to at least one other crystal-like molecule. Adsorbed molecules were defined as disordered molecules that are adjacent to a crystal-like molecule. Solution molecules were all the other disordered molecules. Adsorbed molecules and crystal-like molecules were further numbered as

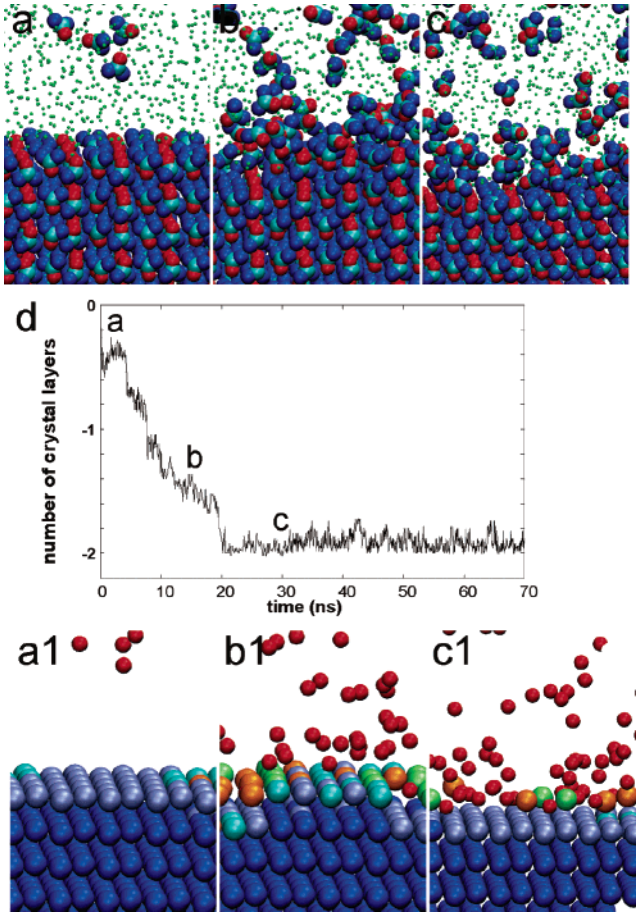

Figure 2. Molecular dynamics simulation of urea dissolution. Snapshots a, b, and c from the simulation correspond to the times 1, 15, and 30 ns, respectively. For the sake of clarity, hydrogen atoms are not shown. (d) Profile of the number of crystal molecules (expressed as number of *xy* lattice planes) during the simulation of the dissolution of the [001] face of urea. Snapshots a1, b1, and c1 are the same samples as those shown in a, b, and c, but in a reduced representation where each molecule is represented by a sphere positioned on the molecular center of mass. Water molecules are not shown. Coloring is as follow: red, solution molecules; orange, adsorbed molecules (A_{1-5}); lime, isolated crystal molecules (C_{1-2}); cyan, kinks and steps (C_{3-4}); ice blue, face (C_5); and blue, bulk crystal (C_6). (See also Figure 1).

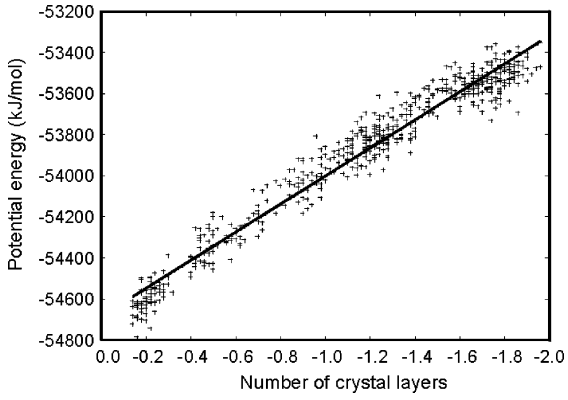

Figure 3. Determination of the urea solvation enthalpy. Plot of the average potential energy as a function of the number of urea molecules in solution. The slope of the curve gives the solvation energy per urea molecule (ΔH_s = 13.7 kJ mol^{-1}). Note that the slope of the plot changes slightly during the MD simulation because of variations in the solution concentration during the MD simulation.

C_1-C_6 and A_1-A_5 according to their number of neighbors (Figure 1), as discussed previously. The following reactions were

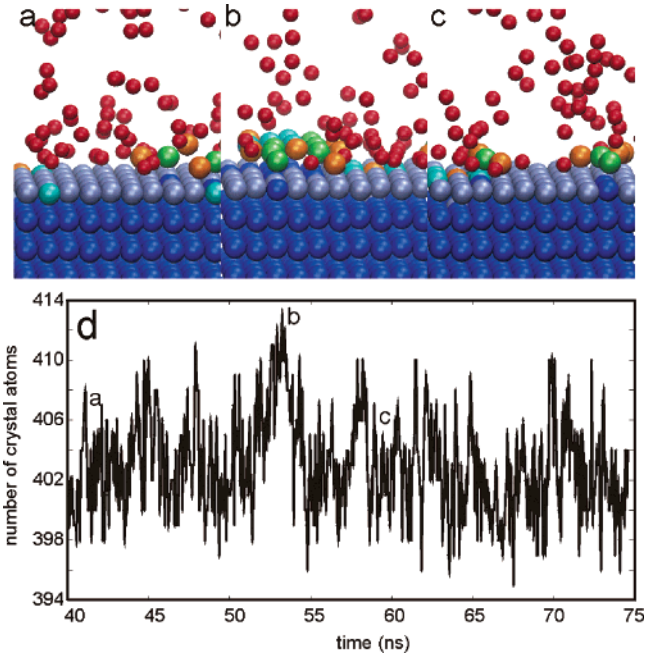

Figure 4. Molecular dynamics simulation of urea solution in contact with the [001] surface. (a, b, c) Snapshots from the simulation. (d) The number of "crystal-like" molecules as a function of time. Note that at t = 12 ns there is the spontaneous formation of a surface crystal nucleus that is stable for approximately 2 ns.

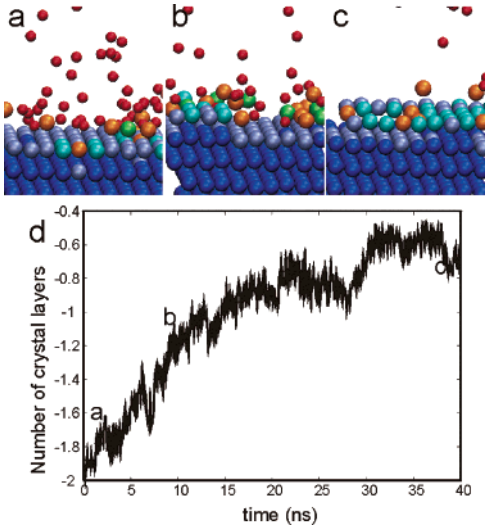

Figure 5. Molecular dynamics simulation at 260 K. (a, b, c) Snapshots from the simulation at t = 2, 10, and 38 ns that illustrate the growth of a new crystal layer during the run. (d) Plot of the number of crystal-like molecules (expressed as number of lattice *xy* planes) as a function of time. Coloring scheme is as per Figure 1.

then postulated to occur: $S \rightleftharpoons A_i$ adsorption of a solute molecule on the surface, $S \rightleftharpoons C_i$ incorporation of a solute molecule in the crystal surface, $A_i \rightleftharpoons A_j$ diffusion of an adsorbed molecule, $A_i \rightleftharpoons C_i$ incorporation of an adsorbed molecule into the crystal, and $C_i \rightleftharpoons C_j$ diffusion of a crystalline molecule. The $A_i \rightleftharpoons C_j$ reactions were decomposed into a combination of a diffusion step plus an incorporation reaction.

The diffusion of crystal-like surface molecules, adsorbed urea molecules, and urea molecules in solution was first investigated (Figure 6). The calculated self-diffusion coefficient for urea molecules in solution at 298 K is 0.0022(2) nm^2 ps^{-1}. This value is in agreement with previous MD simulations[20] and slightly

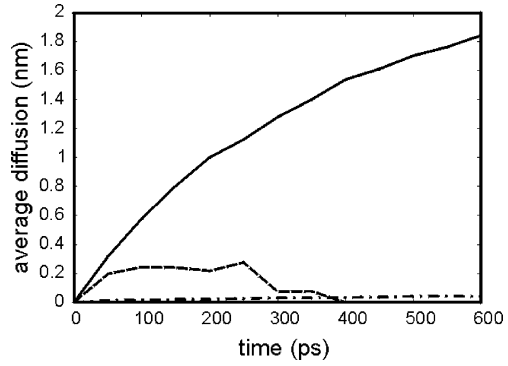

Figure 6. Position−position autocorrelation functions for solution urea molecules (—), adsorbed urea molecules (− − −), and crystal-like urea molecules (− · −).

larger than the experimental value (0.0013 $nm^2\ ps^{-1}$)[30] possibly due to the high diffusivity of SPC water.[20] It turns out that while adsorbed molecules still show a moderate tendency to diffuse during the MD simulation, crystal-like surface molecules diffuse to a negligible extent. For this reason, the probabilities of diffusion on the crystal surface were calculated for adsorbed molecules only. The matrix of the rate constants calculated for all the possible reactions is reported in Table 1. If a value is not present, it means that this event has been observed less than 5 times in the simulation (or has not been observed at all) and it was not possible to calculate a reliable transition probability. From this matrix, the relative energies for all the species and the activation energies can also be calculated and are reported in Tables 2 and 3, respectively. From Table 2, containing the relative energies, it is immediately apparent that the molecules adsorbed on the crystal surface have a higher free energy with respect to molecules in solution or molecules in a crystal-like state. However, Table 3, containing the activation energies, shows that in several cases the lowest energy pathway from the crystal to the solution, and vice versa, involves the formation of a surface-adsorbed intermediate. The variation in activation energy between different paths is often of the order of a few kilojoules per mole, and therefore multiple pathways for the same overall reaction are possible.

The activation energies calculated in Table 3 for the removal of a urea molecule from a clean urea surface can be compared with the free energy calculated from an umbrella sampling simulation with the urea surface distance chosen as a reaction coordinate (Figure 7d). It turns out that the energy calculated from the slowest umbrella sampling simulation (24 kJ mol^{-1}) is very similar to the barrier calculated from the MD simulation transition rates (23(2) kJ mol^{-1}). However, in the umbrella sampling simulations, the total free energy of dissolution of this urea molecule is ∼23 kJ mol^{-1}, as compared to 10(2) kJ mol^{-1} calculated from the transition rates. This is probably because the urea surface distance is a reasonable reaction coordinate for approaching the transition state, but it is a poor reaction coordinate afterward.

It is not an easy task to predict the nature of the crystal growth mechanism for the [001] urea surface from a simple analysis of Tables 1−3. To provide such a description, the data contained within Table 1 have been used as parameters in a lattice-based simulation of crystal growth employing a kinetic Monte Carlo

(30) Gostling, L. J.; Akeley, D. F. *J. Am. Chem. Soc.* **1952**, *74*, 2058−2060.

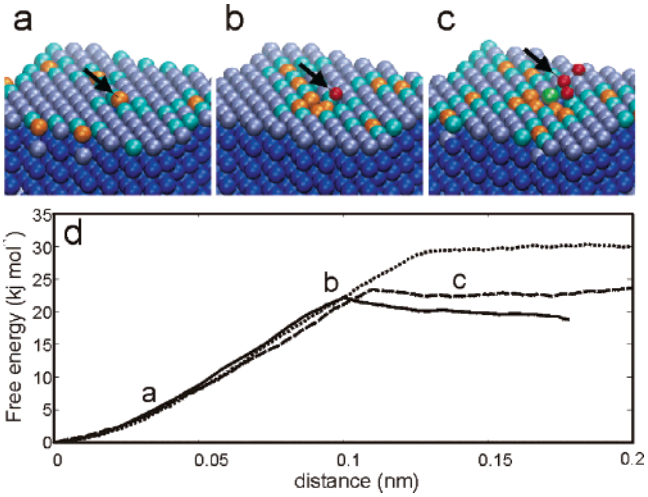

Figure 7. Constrained molecular dynamics simulation of the dissolution of a single molecule from the [001] face. Snapshots a, b and c are samples in reduced representation of the MD simulation corresponding to $d = 0.6$, 1.0, and 1.6 Å, respectively. See caption to Figure 1 for the coloring scheme. (d) Plot of the dissolution free energy as a function of the urea face distance. The three lines correspond to the three pulling speeds employed, with the solid line corresponding to the slowest speed and the dotted the fastest.

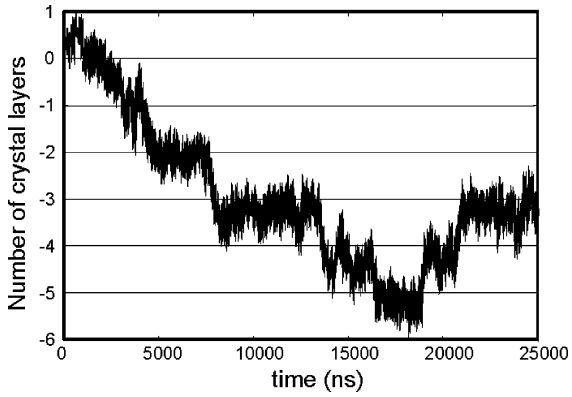

Figure 8. Kinetic Monte Carlo simulation with 64 sites at a relative supersaturation of 0.98. Plot of the number of crystal molecules (expressed as the number of *xy* crystal lattice planes) as a function of time.

algorithm. This makes it feasible to extend the scope of the present work to much larger length scales and longer time scales and to perform simulations at fixed urea concentration. As a first validation step, the dissolution of an 8 × 8 surface in contact with a solution of supersaturation of 0.98 has been studied, where 1.00 is the concentration of the saturated solution in the kinetic Monte Carlo simulation. This simulation reproduces the stepwise dissolution behavior already observed in the classical MD simulation, where only fully formed crystal layers seem to be stable (Figures 2d and 8). The same simulation was then repeated with larger surfaces of size 100 × 100 and 150 × 150, roughly corresponding to areas for the crystal face of 0.025 and 0.056 μm^2. In all of these simulations, the stepwise dissolution that was observed in the 8 × 8 surface simulation is no longer present. This result indicates that this feature is most likely an artifact of the limited size of the classical molecular dynamics simulation.

Finally, we performed a simulation of a 150 × 150 surface in contact with a solution with a supersaturation of 1.02. Figure 9 shows a snapshot from this scenario. Nucleation occurs at several sites, followed by propagation of the nuclei until most of the surface is covered. Nucleation is also observed to occur

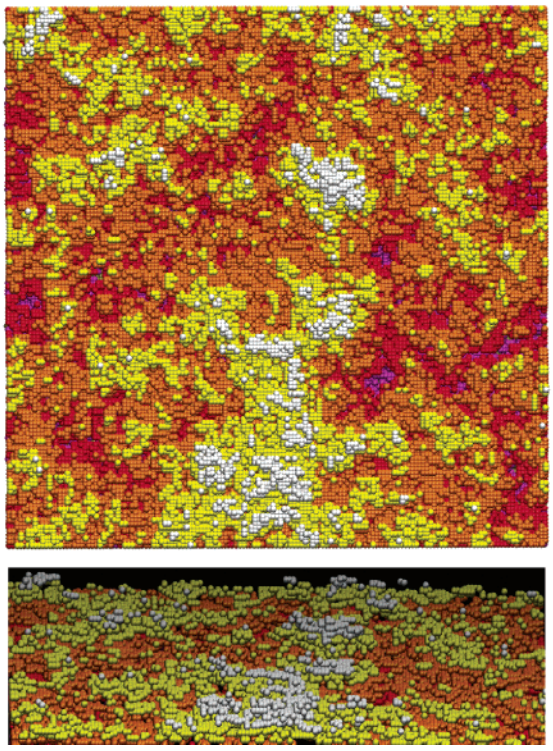

Figure 9. Top and side views of a snapshot from the kinetic Monte Carlo simulation with 22 500 sites at a relative supersaturation of 1.02. Crystal layers have been colored from purple to white according to the layer depth.

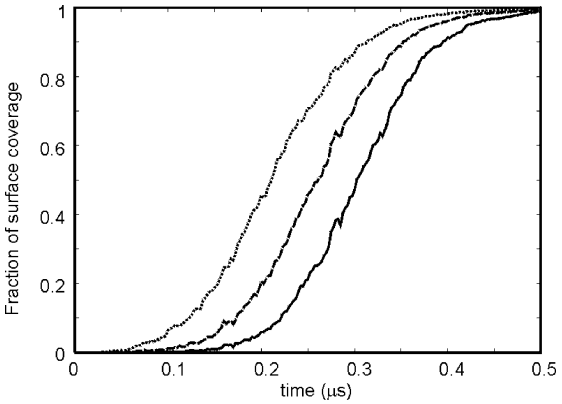

Figure 10. Kinetic Monte Carlo simulation with 22 500 sites at a relative supersaturation of 1.02. Plot of the fraction of coverage for layer 4 (···), layer 5 (– – –), and layer 6 (—).

on incomplete surfaces, leading to a rough surface with islands and pits. Figure 10 shows the degree of surface coverage as a function of time for three subsequent layers. Substantial nucleation on layers 5 and 6 is observed already when the underlying layers 4 and 5 are only 20% covered. After ~0.1 μs of slow growth, the nuclei cover about 5% of the total surface. At this point, the growth speed greatly increases until, after 0.1 μs, 75−80% of the total surface is covered with a new layer. Coverage of the remaining 20% of the surface is a relatively slow process and takes 0.2−0.3 μs. From these observations, we conclude that the overall limiting step is the removal of the residual surface vacancies that occurs at a slower rate compared to the other steps of nucleation and propagation.

Conclusions

Classical molecular dynamics simulations have been utilized to study the atomic level dissolution and growth of the [001] surface of urea in contact with aqueous solution. The dissolution of a single surface later is found to occur rapidly, leading to the formation of a supersaturated solution at 298 K. Once the dissolution is complete, the formation of potential growth nuclei is observed on the surface, and these persist for a few nanoseconds before dispersing again. On cooling to 260 K, thereby reducing the maximum degree of supersaturation, the rapid growth of the surface is found to occur. Growth nuclei are found to form rapidly, as observed during the dissolution process, and evolve leading to an almost complete surface layer. However, the rate-determining step is found to be the removal of surface layer defects, namely pits that contain water instead of urea. This can be understood from the fact that to complete the layer, a water molecule must be removed before urea is adsorbed, which creates a barrier due to the need to locally desolvate the surface.

Through classifying the local environment of each urea molecule during the explicit dynamics, it is possible to construct a lattice-based kinetic Monte Carlo model for surface growth. Conventionally in such work, the activation energies are determined from the potential energy surface and then the rates have to be estimated based on assumptions concerning the prefactors. Because the rates for individual steps are directly determined from the simulations, this ambiguity is avoided during the growth studies, though of course it conversely now becomes an uncertainity in determining the activation energies. Comparison between determination of the activation energy for the first dissolution event and the estimated barrier shows that the assumed prefactors are reasonable for the present system.

Application of the kinetic Monte Carlo scheme to larger surface regions demonstrates that crystal growth is rapid and nucleation is not the rate-limiting factor since successive surface layers begin to form prior to the completion of the underlying layer. Consequently, this leads to the creation of rough surfaces since the removal of defects is slow relative to the surface cluster nucleation rate. Work is now in progress to extend the present study to other surfaces of urea where growth is slower so that the total morphology evolution can be predicted from the growth kinetics.

Acknowledgment. We thank the Government of Western Australia for funding this work under the Premier's Research Fellowship scheme, as well as Curtin University of Technology for provision of computing resources.

JA043395L